Extreme driven ion acoustic waves

L. Friedland[1,a)] and A. G. Shagalov[2,b)]
[1]Racah Institute of Physics, Hebrew University of Jerusalem, Jerusalem 91904, Israel
[2]Institute of Metal Physics, Ekaterinburg 620990, Russian Federation and Ural Federal University, Mira 19, Ekaterinburg 620002, Russian Federation

(Received 1 June 2017; accepted 11 July 2017; published online 1 August 2017)

The excitation of large amplitude, strongly nonlinear ion acoustic waves from trivial equilibrium by a chirped frequency drive is discussed. Under certain conditions, after passage through the linear resonance in this system, the nonlinearity and the variation of parameters work in tandem to preserve the phase-locking with the driving wave via excursion of the excited ion acoustic wave in its parameter space, yielding controlled growth of the wave amplitude. We study these autoresonant waves via a fully nonlinear warm fluid model and predict the formation of sharply peaked (extreme) ion acoustic excitations with local ion density significantly exceeding the unperturbed plasma density. The driven wave amplitude is bound by the kinetic wave-breaking, as the local maximum fluid velocity of the wave approaches the phase velocity of the drive. The Vlasov-Poisson simulations are used to confirm the results of the fluid model, and Whitham's averaged variational principle is applied for analyzing the evolution of autoresonant ion acoustic waves. *Published by AIP Publishing.* [http://dx.doi.org/10.1063/1.4986031]

I. INTRODUCTION

Resonant wave interactions play an important role in plasma applications, examples being plasma based accelerators,[1] stimulated Raman and Brillouin scattering in laser driven plasmas,[2] plasma turbulence,[3] etc. These phenomena require phase matching between the interacting waves, but, frequently, the nonlinear frequency shifts of the interacting waves destroy the phase matching, limiting the amplitude of the excitations. Nevertheless, if the parameters of the plasma or of the driving wave vary slowly in time and/or space, under certain conditions, the resonant wave interaction may continue despite the nonlinearity due to the autoresonance effect,[4] as the interacting waves self-adjust their amplitudes to stay in a persistent nonlinear resonance. In plasmas, supporting a variety of nonlinear waves, this phenomenon was studied for the problem of generation of plasma waves in beat-wave accelerators,[5] in excitation of the diocotron and Bernstein-Green-Kruskal (BGK) modes,[6–8] and stimulated Raman and Brillouin scattering.[9,10] In this paper, we exploit autoresonant wave interactions in the problem of generation of extreme (limited by kinetic wave breaking) ion-acoustic waves.

The ion-acoustic waves (IAWs) in plasmas were predicted by Tonks and Langmuir[11] and observed in experiments by Revans.[12] Since these pioneering works, IAWs were studied in many contexts, such as laser-plasma interactions,[2] ion-acoustic turbulence,[13] and in dusty,[14] ionospheric,[15] ultra-cold,[16] and quantum[17] plasmas. Despite the importance of the IAWs, their theoretical understanding is still incomplete in problems involving a combination of nonlinearity, inhomogeneity or time dependence of the plasma, and kinetic effects. Here, we ask the question of whether one can resonantly excite and control very large amplitude IAWs via the autoresonance effect, i.e., by preserving the phase locking between the driven and driving waves despite the nonlinearity and variation of parameters. Recently, we have addressed the problem of initiation of autoresonant excitation of IAWs within a weakly nonlinear fluid model.[18] We have focused on the case of small ion to electron temperature ratio $\sigma^2 = T_i/T_e \ll 1$ to show that by driving the plasma by a chirped frequency ponderomotive wave passing through the linear ion acoustic resonance, one observes autoresonance in the system if the driving amplitude ε exceeds a sharp threshold $\varepsilon > \varepsilon_{th}$. The threshold has the usual autoresonance scaling $\varepsilon_{th} \sim \alpha^{3/4}$ with the driving frequency chirp rate α.[6] We have also seen numerically[18] that the amplitude of the autoresonant wave in this setting can grow well beyond the weakly nonlinear limit. The present work comprises a fully nonlinear generalization of the theory going beyond the usual Korteweg-de-Vries assumption of $k\lambda_D \ll 1$ and small amplitudes.[19] We will describe the autoresonant growth of the wave amplitude via chirping the driving frequency, allowing a controllable approach to the kinetic wave breaking limit.

The scope of the paper will be as follows. In Sec. II, we will switch to the alternative water bag model of IAWs and illustrate the excitation of extreme (maximal amplitude) waves in simulations. In the same section, we will compare the numerical results of the aforementioned model with the predictions of the associated kinetic Vlasov-Poisson simulations. In Sec. III, we will describe our fully nonlinear theory of driven autoresonant IAWs. The approach will be based on the Whitham's average variational principle[20] using the ideas developed in studying autoresonant excitation and control of other nonlinear waves.[21,22] Finally, Sec. IV will present our conclusions.

II. THE MODEL AND NUMERICAL SIMULATIONS

We model a one-dimensional IAW problem via the waterbag model,[23] i.e., assume a constant ion phase space

a)Electronic mail: lazar@mail.huji.ac.il
b)Electronic mail: shagalov@imp.uran.ru

distribution $f(u,x,t)=\frac{1}{2\Delta}$ between two limiting trajectories $u_{1,2}(x,t)$ and vanishing distribution outside these trajectories.[18] The distribution remains constant between and outside the limiting trajectories as they are deformed in the driven problem and, thus, the waterbag dynamics is governed by the following dimensionless momentum and Poisson equations:

$$\partial_t u_1 + u_1\partial_x u_1 = -\partial_x\phi, \tag{1}$$

$$\partial_t u_2 + u_2\partial_x u_2 = -\partial_x\phi, \tag{2}$$

$$\partial_x^2\phi = e^{\phi+\phi_d} - (u_1-u_2)/2\Delta. \tag{3}$$

Here, we use the time, position and ion fluid velocities $u_{1,2}$ normalized with respect to the inverse ion plasma frequency $\omega_{pi}^{-1}=(m_i/m_e)^{1/2}\omega_p^{-1}$, the Debye length $\lambda_D=u_e/\omega_p$, and the modified electron thermal velocity $(m_e/m_i)^{1/2}u_e$. The plasma density and the electric potential are normalized with respect to the unperturbed plasma density and k_BT_e/e, respectively, while 2Δ measures the initial velocity width of the ion distribution. We also use the assumption of Maxwellian electrons, while the driving (ponderomotive) potential is $\phi_d=\varepsilon\cos\theta_d$, $\varepsilon\ll 1$, and $\theta_d=kx-\int\omega_d dt$, where the driving frequency slowly increases with time, $\omega_d=\omega_0+\alpha t$. Equations (1)–(3) are equivalent to a more conventional fluid system,

$$\partial_t n + \partial_x(un) = 0, \tag{4}$$

$$\partial_t u + uu_x = -\partial_x\phi - 3\sigma^2 n\partial_x n, \tag{5}$$

$$\partial_x^2\phi = \exp(\phi+\phi_d) - n. \tag{6}$$

with the adiabatic ion pressure scaling $p\sim n^3$ and $\sigma^2=T_i/T_e$ being the ratio of the ion and electron temperatures. The transition between the two models is accomplished by setting $\Delta^2=3\sigma^2$ and relating

$$u=(u_1+u_2)/2, \tag{7}$$

$$n=(u_1-u_2)/2\Delta. \tag{8}$$

We illustrate the excitation of a chirped-driven IAW by solving Eqs. (1)–(3) numerically using a standard pseudospectral method,[24] subject to uniform initial and periodic boundary conditions $u_{1,2}(x,0)=\pm\Delta$, $\phi(x,0)=0$, $u_{1,2}(x+L,t)=u_{1,2}(x,t)$, $\phi(x+L,t)=\phi(x,t)$, $L=2\pi/k$ and parameters $\sigma=0.05$, $k=0.5$, $\varepsilon=0.008$, $\alpha=0.0002$. The driving frequency $\omega_d=\omega_0+\alpha t$ is swept from below through the linear IAW wave frequency

$$\omega_0 = k\sqrt{\Delta^2+\frac{1}{1+k^2}} \tag{9}$$

in the problem. Figure 1 shows the spatial distribution of the density n [panel (a)] and potential ϕ [panel (b)] of the wave (in the wave frame) at three values of slow time $\tau=\sqrt{\alpha}t$, i.e., $\tau=0$ (at the linear resonance), $\tau=4$, and $\tau=8$ by starting at $\tau=-10$. Note that the density develops a sharply peaked spatial profile, with the maximum ion density at $\tau=8$ reaching nearly twice the unperturbed density ($n_0=1$). Additional details of the excitation process are shown in Fig. 2, where panel (a) presents the time evolution of the maximum value of the density wave, while panel (b) shows

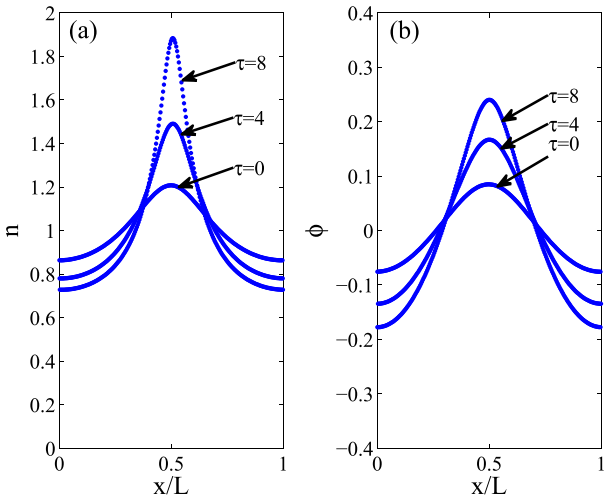

FIG. 1. The spatial profile of the autoresonant ion acoustic wave (in wave frame) during the excitation process at three different values of slow time $\tau=0,4,8$. (a) The ion density n and (b) the wave potential ϕ.

the evolution of the phase mismatch between the driven and driving waves. The driving frequency in Figs. 1 and 2 is chirped linearly in time until $\tau=8$ and remains constant for $\tau>8$. One can see that the system phase locks in passing the linear resonance and that the phase locking continues (the system is in autoresonance), while the wave amplitude increases in average during the chirped stage of excitation. The phase locking also persists after the chirp is switched off, and at all stages of excitation both the wave amplitude and the phase mismatch exhibit slow oscillating modulations around the average, indicating modulational stability in the problem. We have also compared the results of our simulations of Eqs. (1)–(3) with full kinetic simulations of the associated Vlasov-Poisson system[18]

$$f_t + uf_x + \phi_x f_u = 0, \quad \phi_{xx} = \exp(\phi+\phi_d) - \int f du, \tag{10}$$

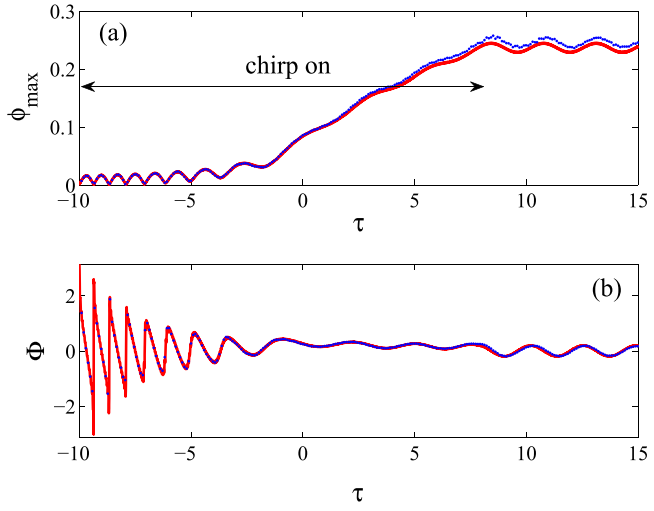

FIG. 2. The maximum of the ion acoustic wave potential ϕ_{max} [panel (a)] and the phase mismatch between the driven and driving waves [panel (b)] versus slow time τ. The drive is still on after $\tau=8$, but its frequency chirp is off. The waterbag model is represented by full red lines and Vlasov-Poisson simulations are shown by dotted blue lines.

where initially $\phi(x,0)=0$ and $f(x,u,0)=(2\pi\sigma^2)^{-1/2}\exp(-u^2/2\sigma^2)$. The results of these simulations are shown by dots in Fig. 2, showing excellent agreement with the waterbag model, while the actual ion phase space distribution $f(x,u,\tau)$ associated with the excited IAW in this example at $\tau=8$ is shown in Fig. 3(a). For comparison, Fig. 3(b) shows the corresponding waterbag distribution. The figure illustrates the proximity to the kinetic wave breaking limit at this τ, as some particles in the spatial peak of the distribution have velocities close to the phase velocity ($v_d=0.709$) of the driving wave. We find numerically that if the chirp of the driving frequency is continued beyond $\tau=8$, the phase locking and stability of the excited wave are destroyed. Finally, we have also tried a driving protocol (not illustrated in the figures), where after the autoresonant excitation stage, instead of terminating the driving frequency chirp at $\tau=8$, we set $\varepsilon=0$, i.e., switched the drive off for $\tau>8$. The result was a free, stable large amplitude IAW with frequency close to the final frequency of the drive. Next, we proceed to the theory of chirped-driven IAWs.

III. FULLY NONLINEAR THEORY OF AUTORESONANT ION-ACOUSTIC WAVES

Our theory is based on the waterbag model (1)–(3), where we define potentials $\psi_{1,2}$ via $u_{1,2}=\partial_x\psi_{1,2}$ and assume a weak drive

$$\begin{aligned}&\partial_{tx}^2\psi_1+\partial_x\psi_1\partial_{xx}^2\psi_1=-\partial_x\phi,\\&\partial_{tx}^2\psi_2+\partial_x\psi_2\partial_{xx}^2\psi_2=-\partial_x\phi,\\&\partial_{xx}^2\phi=e^{\phi}(1+\phi_d)-(\partial_x\psi_1-\partial_x\psi_2)/2\Delta.\end{aligned}\tag{11}$$

This system can be obtained via the variation principle $\delta(\int L dx dt)=0$, with the three-field Lagrangian density $L=L_0+L_1$, where

$$\begin{aligned}L_0=&\frac{1}{2}(\partial_x\phi)^2+e^{\phi}-\frac{(\partial_x\psi_1\partial_t\psi_1-\partial_x\psi_2\partial_t\psi_2)}{4\Delta}\\&-\frac{(\partial_x\psi_1)^3-(\partial_x\psi_2)^3}{12\Delta}-\frac{(\partial_x\psi_1-\partial_x\psi_2)\phi}{2\Delta}\end{aligned}\tag{12}$$

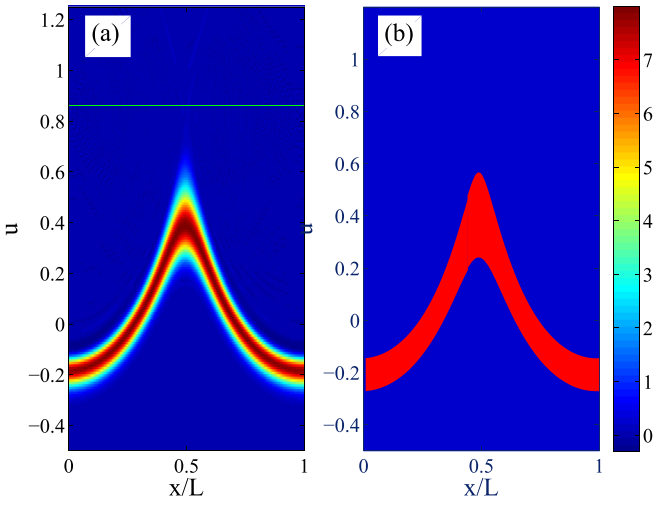

FIG. 3. The ion phase space distribution at the final time, $\tau=15$, in the example in Figs. 1 and 2; (a) The full kinetic simulations and (b) the waterbag model. The horizontal line in panel (a) shows the final location of the phase velocity of the driving wave.

and $L_1=e^{\phi}\phi_d$. We seek solutions of form $\phi=\phi(\theta)$, $\psi_{1,2}=\beta_{1,2}x+V_{1,2}(\theta)$, where $\phi(\theta)$ and $V_{1,2}(\theta)$ are 2π-periodic in the fast phase $\theta=kx-\int\Omega dt$, while $\beta_{1,2}$ are constant and Ω is the slow frequency reflecting the slow frequency chirp of the drive. We also assume that $\phi(\theta)$ and $\partial_xV_{1,2}(\theta)$ have zero θ-averages, yielding $\beta_{1,2}=\pm\Delta$. Next, we replace $\partial_x\psi_{1,2}=\beta_{1,2}+\partial_xV_{1,2}$ and $\partial_t\psi_{1,2}=-v_p\partial_xV_{1,2}$ in the Lagrangian density ($v_p=\Omega/k$ being the wave phase velocity) and drop the terms which do not include field variables. This yields the unperturbed Lagrangian density

$$\begin{aligned}L_0=&\frac{1}{2}(\partial_x\phi)^2-\phi+e^{\phi}-\frac{(\Delta-v_p)}{4}\left[\frac{(\partial_xV_1)^2}{\Delta}+\partial_xV_1\right]\\&-\frac{(\Delta+v_p)}{4}\left[\frac{(\partial_xV_2)^2}{\Delta}+\partial_xV_2\right]\\&-\frac{(\partial_xV_1)^3-(\partial_xV_2)^3}{12\Delta}-\frac{(\partial_xV_1-\partial_xV_2)\phi}{2\Delta}.\end{aligned}\tag{13}$$

For fixed v_p, the problem described by L_0 is integrable. Indeed, we have two constant canonical momenta $p_{1,2}=\partial L_0/\partial(\partial_xV_{1,2})$,

$$p_1=-\frac{\phi}{2\Delta}-\frac{(\Delta-v_p)}{4}\left(\frac{2\partial_xV_1}{\Delta}+1\right)-\frac{(\partial_xV_1)^2}{4\Delta},\tag{14}$$

$$p_2=\frac{\phi}{2\Delta}-\frac{(\Delta+v_p)}{4}\left(\frac{2\partial_xV_2}{\Delta}-1\right)+\frac{(\partial_xV_2)^2}{4\Delta},\tag{15}$$

which can be used to express

$$\partial_xV_1=v_p-\Delta-s_1,\tag{16}$$

$$\partial_xV_2=v_p+\Delta-s_2,\tag{17}$$

where

$$s_{1,2}=\sqrt{2(B_{1,2}-\phi)}.\tag{18}$$

In the definition of $s_{1,2}$, we use new conserved parameters, $B_{1,2}$, instead of $p_{1,2}$

$$B_1=\frac{v_p}{2}(v_p-\Delta)-2p_1\Delta,\tag{19}$$

$$B_2=\frac{v_p}{2}(v_p+\Delta)+2p_2\Delta.\tag{20}$$

Note that initially, ($\phi=\partial_xV_1=\partial_xV_2=0$), $p_1=(v_p-\Delta)/4, p_2=(v_p+\Delta)/4, B_1=(v_p-\Delta)^2/2$, and $B_2=(v_p+\Delta)^2/2$. The choice of the signs at $s_{1,2}$ in (16) and (17) is such that $\partial_xV_{1,2}=0$ initially. In addition to $B_{1,2}$, the energy function

$$A'=(\partial_x\phi)^2+p_1\partial_xV_1+p_2\partial_xV_2-L_0\tag{21}$$

is also conserved in the fixed v_p case. Then, by substituting (19), and (20) in (21), we get the usual energy conservation-type equation

$$\frac{1}{2}\phi_x^2+U_{eff}=A,\tag{22}$$

where the effective potential is

$$U_{eff} = -\frac{1}{2}v_p^2 - \frac{B_1}{2\Delta}(v_p - \Delta) + \frac{B_2}{2\Delta}(v_p + \Delta) + \frac{s_1^3 - s_2^3}{6\Delta} - e^{\phi} + 1 - \frac{\Delta^2}{6} \tag{23}$$

and $A = A' + 1 - \Delta^2/6$. We have added $1 - \Delta^2/6$ to A' to make the effective potential zero for the initially unperturbed ($\phi = 0$) plasma. Indeed, initially, $p_1 = (v_p - \Delta)/4, p_2 = (v_p + \Delta)/4$ and $B_1 = (v_p - \Delta)^2/2$, $B_2 = (v_p + \Delta)^2/2$, and by expanding U_{eff} in ϕ to second order, we get

$$U_{eff} = \frac{1}{2}\left(1 - \frac{1}{v_p^2 - \Delta^2}\right)\phi^2 + O(\phi^3). \tag{24}$$

Then, the spatial frequency (i.e., k) of small oscillations of ϕ is

$$k = \sqrt{\frac{1}{v_p^2 - \Delta^2} - 1} \tag{25}$$

in agreement with the linear dispersion relation (9). Next, following Whitham's procedure,[10] we average (21) over θ to obtain the averaged Lagrangian density $\Lambda_0 = \langle L_0 \rangle_\theta$

$$\Lambda_0(A, B_1, B_2; v_p) - 1 + \Delta^2/6 = \langle (\partial_x \phi)^2 \rangle - A = kI(A, B_1, B_2; v_p) - A, \tag{26}$$

where

$$I = \frac{1}{2\pi k}\int_0^{2\pi} \phi_x^2 d\theta = \frac{1}{2\pi}\oint [2(A - U_{eff})]^{1/2} d\phi. \tag{27}$$

is the usual action integral. The perturbed part of the averaged Lagrangian density is

$$\Lambda_1 = \langle e^{\phi}\phi_d \rangle_\theta = \frac{\varepsilon}{2}a_1(I)\cos\Phi, \tag{28}$$

where we have expanded $e^{\phi} = \sum a_n(I)\cos(n\theta)$, neglected all but fundamental harmonic in this expansion (this is the isolated resonance approximation[25]), wrote $\theta_d = \theta - \Phi$, and assumed a slow phase mismatch Φ in the problem. Then, the full averaged Lagrangian density is

$$\Lambda = kI(A, B_1, B_2; v_p) - A + \frac{\varepsilon}{2}a_1(I)\cos\Phi. \tag{29}$$

This Lagrangian density can be used by taking variations with respect to A, B_1, B_2, and θ to yield

$$k\partial_A I - 1 + \frac{\varepsilon}{2}\partial_A a_1 \cos\Phi = 0, \tag{30}$$

$$k\partial_{B_1} I + \frac{\varepsilon}{2}\partial_{B_1} a_1 \cos\Phi = 0, \tag{31}$$

$$k\partial_{B_2} I + \frac{\varepsilon}{2}\partial_{B_2} a_1 \cos\Phi = 0, \tag{32}$$

and

$$\frac{d}{dt}(\partial_{v_p} I) = \frac{\varepsilon}{2}a_1(I)\sin\Phi. \tag{33}$$

With the addition of

$$\frac{d\Phi}{dt} = \Omega - \omega_d(t), \tag{34}$$

we now have a complete system of slow equations for A, B_1, B_2, Ω, and Φ. The phase-locked quasi-equilibrium $\Phi \approx 0$ in this system is obtained via solving a simpler set of three algebraic equations for A, B_1, B_2

$$k\partial_A I - 1 \approx 0, \tag{35}$$

$$\partial_{B_1} I \approx 0, \tag{36}$$

$$\partial_{B_2} I \approx 0, \tag{37}$$

where $\Omega = \omega_d(t)$.

To check our theory in a simplified problem, take the limit $\Delta \to 0$ and consider the undriven case, with v_p being the phase velocity of the undriven wave. Furthermore, assume $B_1 = (v_p - \Delta)^2/2$ and $B_2 = (v_p + \Delta)^2/2$, as for the linear equilibrium. In this case, $(B_1 + B_2)/2 \to v_p^2/2$, $v_p(B_1 - B_2)/2\Delta \to -v_p^2$, and

$$(s_1^3 - s_2^3)/6\Delta \to \frac{3s^2}{6}\frac{s_1 - s_2}{B_1 - B_2}\frac{B_1 - B_2}{\Delta} \to -\frac{v_p s^2}{2}\frac{\partial s}{\partial B} = -v_p s, \tag{38}$$

where $s = \sqrt{v_p^2 - 2\phi}$. Then, Eq. (23) yields the well-known Sagdeev potential for the IAWs[26]

$$U_{eff} \to v_p^2 - v_p\sqrt{v_p^2 - 2\phi} - e^{\phi} + 1. \tag{39}$$

In this case, $I = I(A, v_p)$ and Eq. (35) yields the nonlinear dispersion relation $v_p = v_p(A)$ of the wave. In contrast to this well-known problem, in the chirped autoresonant case, we cannot assume that $B_{1,2}$ and A remain constant during the evolution. In the quasi-static approximation, these slow variables are described by Eqs. (35)–(37) for a given dependence of the driving frequency ω_d on time. We present an example of such calculations in the case of $\sigma = 0.03$ and driving parameters $k = 1$, $\varepsilon = 0.008$, and $\alpha = 0.0001$. Figure 4 shows (thick lines) the evolution of the quasi-energy A and slow

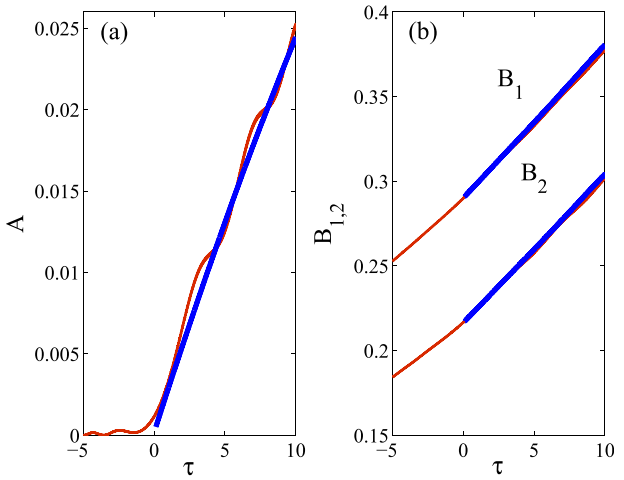

FIG. 4. An example of the time evolution of the quasi-energy A and slow parameters $B_{1,2}$ from the averaged Lagrangian theory (thick blue lines) and from the full fluid simulations (thinner red lines).

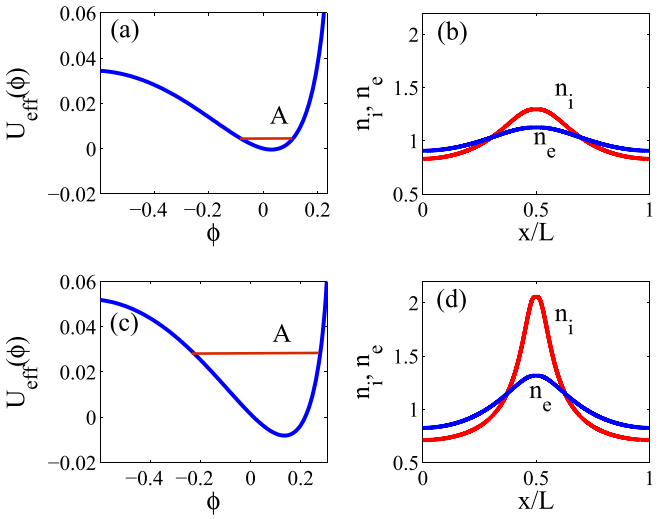

FIG. 5. The effective potential $U_{eff}(\phi)$ and the spatial distribution of the densities of plasma species $n_{i,e}$ from the averaged Lagrangian theory at two times $\tau = 2$ [panels (a) and (b)] and $\tau = 10$ [panels (c) and (d)]. The parameters in these examples correspond to those of Fig. 4 and the horizontal red lines in panels (a) and (c) show the value of the quasi-energy A at the corresponding times.

parameters $B_{1,2}$ obtained by solving the algebraic system (35)–(37) numerically. In the same figure, the numerical results from the full fluid system (1)–(3) are shown by thin lines. One observes a good agreement beyond the linear resonance, the discrepancy due to the neglect of ε in (35)–(37). One can also see oscillating modulations of A and $B_{1,2}$ in fluid simulations around the quasi-equilibrium. As mentioned earlier, these modulations are characteristic of many autoresonant problems and reflect the modulational stability of the autoresonant evolution. Their detailed analysis requires the numerical solution of Eqs. (30)–(34), which is beyond the scope of this paper. Additional results from the variational theory in our example are presented in Fig. 5, which shows the quasi-potential U_{eff} [Figs. 5(a) and 5(c)], and the ion and electron densities n and $\exp(\phi)$ versus x/L [Figs. 5(b) and 5(d)] for two values of the driving phase velocity $v_p = 0.75$ and 0.82. The corresponding quasi-energies A for these values of v_p are represented by horizontal red lines in the figure. The development of a sharply peaked density profile in the figure is associated with the approach of the quasi-energy to the value at which the parameter $s_1 = \sqrt{2(B_1 - \phi)}$ vanishes. As mentioned earlier, the kinetic effects limit this development. This completes the discussion of our averaged variational approach to autoresonant IAWs and we proceed to conclusions.

IV. CONCLUSIONS

We have studied the excitation and control of large amplitude IAWs by a chirped frequency driving wave. The process involved passage through linear resonance in the problem and transition to the autoresonant stage of excitation, where the driven IAW self-adjusted its parameters (both its amplitude and frequency increased) to stay in continuous resonance with the drive. The method allowed reaching extreme excitation amplitudes as the ion density developed a sharply peaked spatial profile with the maximum exceeding the unperturbed ion density significantly. At later stages of excitation, when the local maximum of the ion fluid velocity approached the phase velocity of the driving wave, the autoresonant process discontinued due to the kinetic wave breaking. These predictions were confirmed in numerical simulations using the waterbag model [see Eqs. (1)–(3)] and compared with fully kinetic Vlasov-Poisson simulations [Eqs. (10)]. We have also developed the adiabatic theory for studying the formation of autoresonant IAWs. The theory used Whitham's averaged Lagrangian approach applied to the waterbag model. It allowed interpretation of the driven IAWs as a dynamical problem of an oscillation of a quasi-particle in a slowly evolving effective potential (generalization of the Sagdeev potential). The evolution of the energy of the quasi-particle and other slow parameters of this dynamics can be found by solving adiabatic Eqs. (30)–(34). We have applied this theory in studying the quasi-static evolution of the IAWs in the problem [this case reduces to solving algebraic Eqs. (35)–(37)] and illustrated a good agreement with simulations. The averaged Lagrangian approach is suitable for studying the stability of the extreme IAW excitations as seen in simulations, which seems to be an important goal for the future. We have identified the kinetic wave breaking process as responsible for terminating the autoresonant excitation of IAWs, and limiting the amplitude of the excited IAW. In seeking even larger amplitude excitations, one must avoid this kinetic wave breaking by decreasing the ion temperature. Alternatively, this goal can be reached in higher Z (ion charge) plasmas, where the linear ion acoustic frequency increases by a factor of $Z^{1/2}$, distancing the driving frequency necessary for autoresonant excitation from the ion velocity distribution. Investigation of these effects, as well as a study of the details of the kinetic wave breaking process for application to autoresonant IAWs also comprise important goals for future research.

ACKNOWLEDGMENTS

This work was supported by the Israel Science Foundation Grant No. 30/14.

[1]T. Tajima and J. M. Dawson, Phys. Rev. Lett. **43**, 267 (1979).
[2]W. L. Kruer, *The Physics of Laser-Plasma Interactions* (Addison-Wesley, New York, 1988).
[3]R. Z. Sagdeev and A. A. Galeev, *Nonlinear Plasma Theory* (W. A. Benjamin, New York, 1969).
[4]L. Friedland, Phys. Rev. Lett. **69**, 1749 (1992).
[5]R. R. Lindberg, A. E. Chapman, J. S. Wurtele, and L. Friedland, Phys. Rev. Lett. **93**, 055001 (2004).
[6]J. Fajans, E. Gilson, and L. Friedland, Phys. Rev. Lett. **82**, 4444 (1999).
[7]W. Bertsche, J. Fajans, and L. Friedland, Phys. Rev. Lett. **91**, 265003 (2003).
[8]L. Friedland, P. Khain, and A. G. Shagalov, Phys. Rev. Lett. **96**, 225001 (2006).
[9]O. Yaakobi, L. Friedland, R. R. Lindberg, A. E. Charman, G. Penn, and J. S. Wurtele, Phys. Plasmas **15**, 032105 (2008).
[10]E. A. Williams, B. I. Cohen, L. Divol, M. R. Dorr *et al.*, Phys. Plasmas **11**, 231 (2004).
[11]L. Tonks and I. Langmuir, Phys. Rev. **33**, 195 (1929).
[12]R. W. Revans, Phys. Rev. **44**, 798 (1933).
[13]V. Y. Bychenkov, V. P. Silin, and S. A. Uryupin, Phys. Rep. **164**, 119 (1988).
[14]P. K. Shukla and A. A. Mamun, New J. Phys. **5**, 17 (2003).

[15]J. Pavan, L. F. Ziebell, P. H. Yoon, and R. Gaelzer, J. Geophys. Res. **115**, A02310, doi:10.1029/2009JA014448 (2010).
[16]J. Castro, P. McQuillen, and T. C. Killian, Phys. Rev. Lett. **105**, 065004 (2010).
[17]F. Haas, L. G. Garcia, J. Goedert, and G. Manfredi, Phys. Plasmas **10**, 3858 (2003).
[18]L. Friedland and A. G. Shagalov, Phys. Rev. E **89**, 053103 (2014).
[19]D. R. Nicholson, *Introduction to Plasma Theory* (Wiley, New York, 1983) p. 171.
[20]G. B. Whitham, *Linear and Nonlinear Waves* (Wiley, New York, 1974).
[21]L. Friedland and A. G. Shagalov, Phys. Rev. E **71**, 036206 (2005).
[22]L. Friedland and A. G. Shagalov, Phys. Rev. Lett. **81**, 4357 (1998).
[23]H. L. Berk, C. E. Nielsen, and K. V. Roberts, Phys. Fluids **13**, 980 (1970).
[24]C. Canuto, M. Y. Hussaini, A. Quarteroni, and T. A. Zang, *Spectral Methods in Fluid Dynamics* (Springer-Verlag, New York, 1988).
[25]B. V. Chirikov, Phys. Rep. **52**, 263 (1979).
[26]F. F. Chen, *Introduction to Plasma Physics and Controlled Fusion* (Plenum Press, New York, 1984), p. 299.